Michigan Technological University

Digital Commons @ Michigan Tech

Michigan Tech Patents

Vice President for Research Office

10-4-2005

Magneto-photonic crystal isolators

Miguel Levy
Michigan Technological University, mlevy@mtu.edu

Follow this and additional works at: https://digitalcommons.mtu.edu/patents

Part of the Electromagnetics and Photonics Commons

Follow this and additional works at: https://digitalcommons.mtu.edu/patents

Part of the Electromagnetics and Photonics Commons

(12) **United States Patent**
Levy

(10) **Patent No.:** US 6,952,300 B2
(45) **Date of Patent:** Oct. 4, 2005

(54) **MAGNETO-PHOTONIC CRYSTAL ISOLATORS**

(75) Inventor: **Miguel Levy**, Chassell, MI (US)

(73) Assignee: **Board of Control of Michigan Technological University**, Houghton, MI (US)

(*) Notice: Subject to any disclaimer, the term of this patent is extended or adjusted under 35 U.S.C. 154(b) by 0 days.

(21) Appl. No.: **10/469,436**

(22) PCT Filed: **Feb. 27, 2002**

(86) PCT No.: **PCT/US02/05921**

§ 371 (c)(1),
(2), (4) Date: **Aug. 28, 2003**

(87) PCT Pub. No.: **WO02/069029**

PCT Pub. Date: **Sep. 6, 2002**

(65) **Prior Publication Data**

US 2004/0080805 A1 Apr. 29, 2004

Related U.S. Application Data

(60) Provisional application No. 60/272,100, filed on Feb. 28, 2001.

(51) **Int. Cl.^{7}** **G02F 1/09**; G02F 1/00; G02F 1/295

(52) **U.S. Cl.** **359/280**; 359/324; 385/6

(58) **Field of Search** 359/280–282, 359/237–240, 324, 484; 369/13.1; 385/6

(56) **References Cited**

U.S. PATENT DOCUMENTS

4,375,910 A	3/1983	Seki
4,806,885 A	2/1989	Morimoto
4,932,760 A	6/1990	Arii et al.
4,974,944 A	12/1990	Chang
4,981,341 A	1/1991	Brandle, Jr. et al.
4,995,696 A	2/1991	Nishimura et al.

5,031,983 A	7/1991	Dillon, Jr. et al.
5,040,863 A	8/1991	Kawakami et al.
5,146,361 A	9/1992	Licht
5,151,955 A	9/1992	Ohta et al.
5,237,445 A	8/1993	Kuzuta
5,408,354 A	4/1995	Hosokawa
5,446,578 A	8/1995	Chang et al.
5,479,290 A	12/1995	Tanno et al.
5,774,264 A	6/1998	Konno et al.
5,785,752 A	7/1998	Tanno et al.
5,808,793 A	9/1998	Chang et al.
6,075,642 A	6/2000	Chang
6,262,949 B1	7/2001	Inoue et al.
6,545,795 B2	4/2003	Matsushita et al.
2002/0018913 A1	2/2002	Kato et al.
2002/0063941 A1	5/2002	Matsushita et al.

OTHER PUBLICATIONS

M. Inoue, et al., "Magneto–Optical Properties of One–Dimensional Photonic Crystals Composed of Magnetic and Dielectric Layers," J. Appl. Phys. 83, No. 11, 6768–6770, Jun. 1998.
M. Inoue, et al., "A Theoretical Analysis of Magneto–Optical Faraday Effect of YIG Films with Random Multilayer Structures," J. Appl. Phys. 81, No. 8, 5659–5661, Apr. 1997.
M. Inoue, et al., "One–Dimensional Magnetophotonic Crystals," J. Appl. Phys. 85, No. 8, 5768–5770, Apr. 1999.

(Continued)

Primary Examiner—Loha Ben
Assistant Examiner—Jack Dinh
(74) *Attorney, Agent, or Firm*—Michael Best & Friedrich LLP

(57) **ABSTRACT**

A magneto-optical isolator (20) for an optical circuit. The isolator includes a substrate, and an optical channel (350) disposed next to the substrate. The optical channel and substrate are configured to transmit optical radiation within the optical channel. The isolator further includes a photonic-crystal rotator (24) formed with the substrate and the optical channel. The rotator has at least one defect (52) and magnetic (M) and non-magnetic (N) materials.

17 Claims, 7 Drawing Sheets
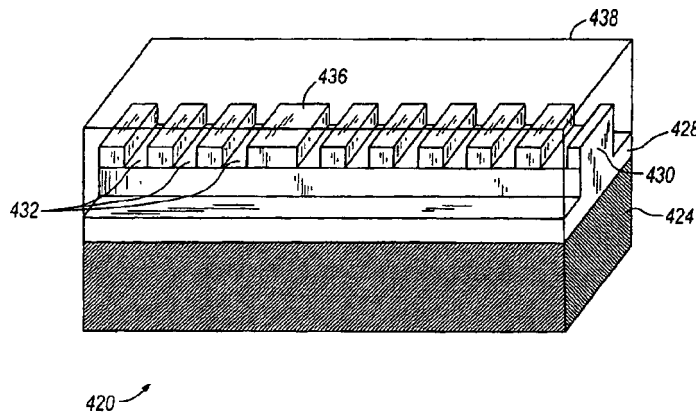
OTHER PUBLICATIONS

E. Takeda, et al., "Faraday Effect Enhancement in Co–Ferrite Layer Incorporated Into One–Dimensional Photonic Crystal Working as a Fabry–Perot Resonator," J. Appl. Phys. 87, No. 9, 6782–6784, May 2000.

S. Sakaguchi, et al., "Transmission Properties of Multilayer Films Composed of Magneto–Optical and Dielectric Materials," IEEE J. Lightwave Technol., 17, No. 6, 1087–1999, Jun. 1999.

M. J. Steel, et al., "High Transmission Enhanced Faraday Rotation in One–Dimensional Photonic Crystals with Defects," IEEE Photonics Technol. Lett. 12, No. 9, 1171–1173, Sep. 2000.

M. J. Steel, et al., "Large Magneto–Optical Kerr Rotation with High Reflectivity from Photonic Band Gap Structures with Defects," IEEE J. Lightwave Technol. 18, No. 9, 1289–1296, Sep. 2000.

M. J. Steel, et al., "Photonic Band Gaps with Defects and the Enhancement of Faraday Rotation," IEEE J. Lightwave Technol. 18, No. 9, 1297–1308, Sep. 2000.

Toshihiro Shintaku, et al., "Magneto–Optic Channel Waveguides in Ce–Substituted Yttrium Iron Garnet," J. Appl. Phys. 74, No. 8, 4877–4881, Oct. 1993.

Wei Li, et al., "Phase–Shifted Bragg Grating Filters with Symmetrical Structures," IEEE J. Lightwave Technol. 15, 1405–1409, Aug. 1997.

M. Levy, et al., "Flat Top Response in One–Dimensional Magnetic Photonic Band Gap Structures with Faraday Rotation Enhancement," IEEE J. Lightwave Technol. 19, 1964–1969 (2001).
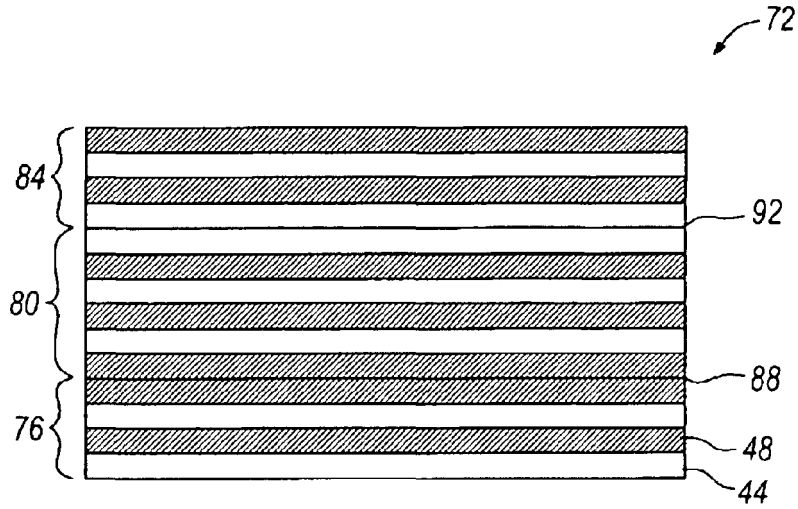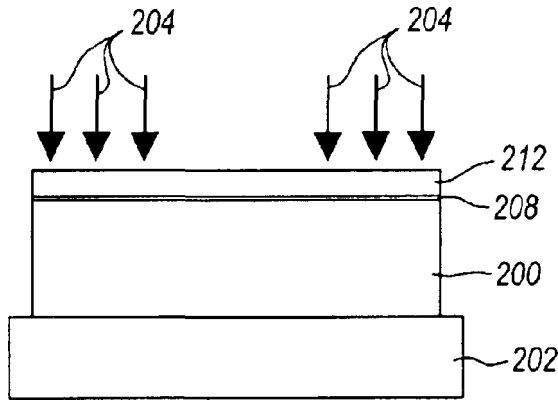
FIG. 1

FIG. 2

FIG. 3

72

84 {
92

80 {
88

76 {
48
44

FIG. 4

204   204

212
208

200

202

FIG. 12

216

0030 25K   50um
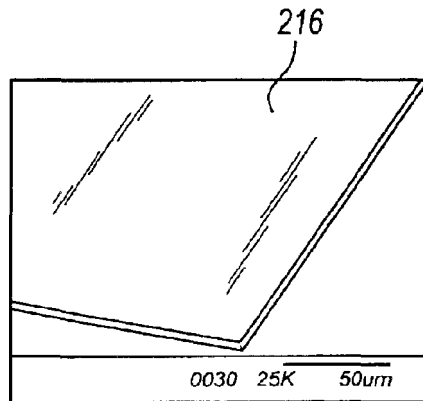
FIG. 13
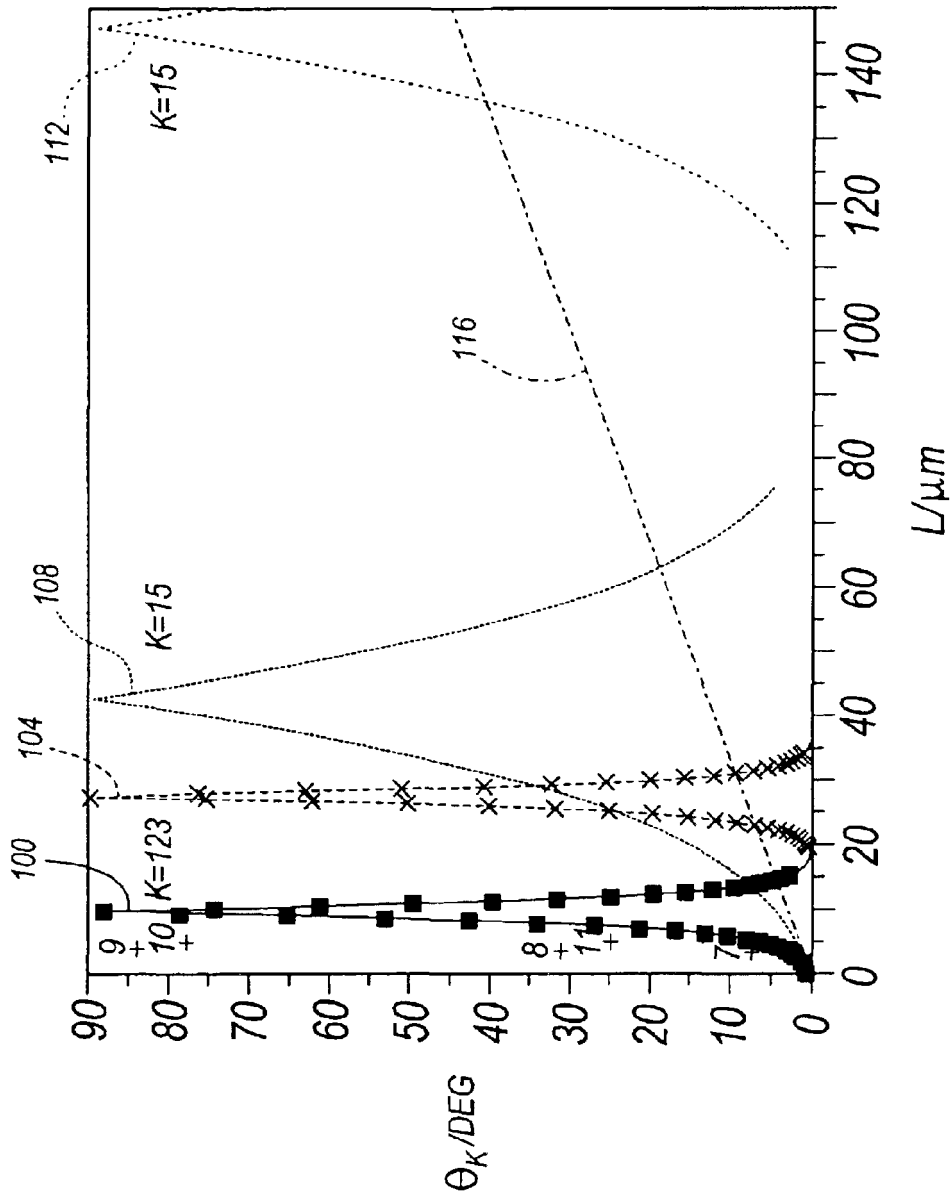
FIG. 5
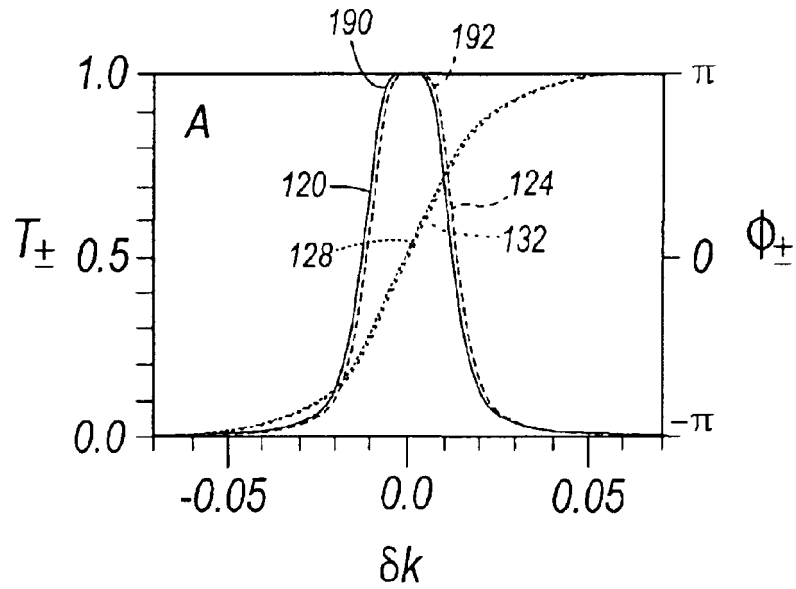
FIG. 6
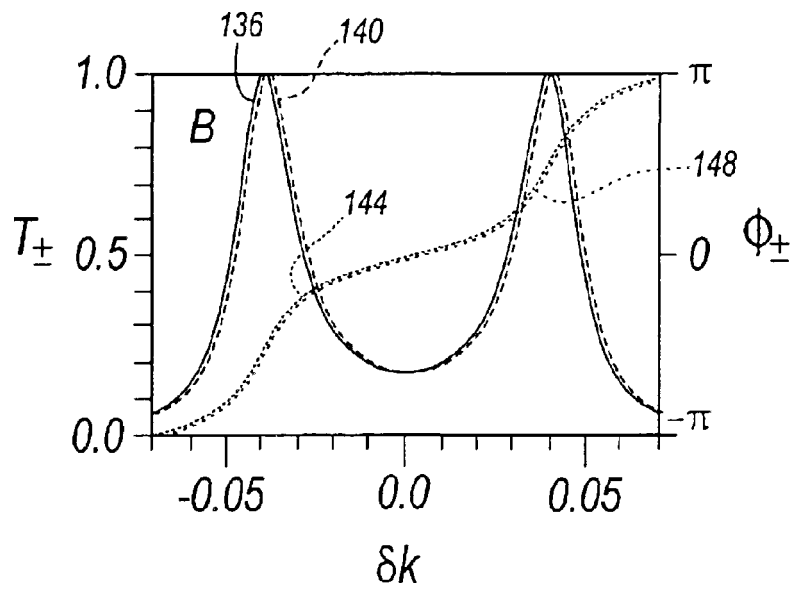
FIG. 7

FIG. 8

FIG. 9

FIG. 10

FIG. 11

438

436

428

430

432

424

420

FIG. 14

440   444

430

428
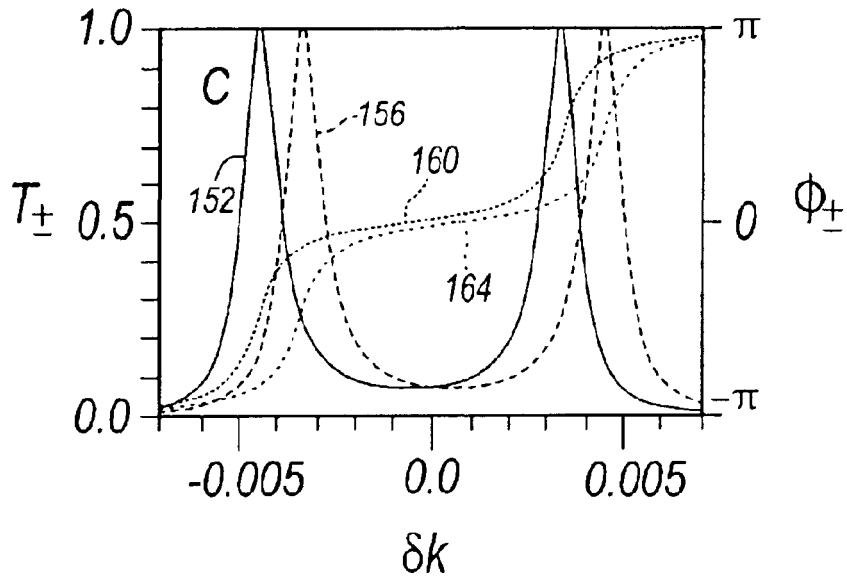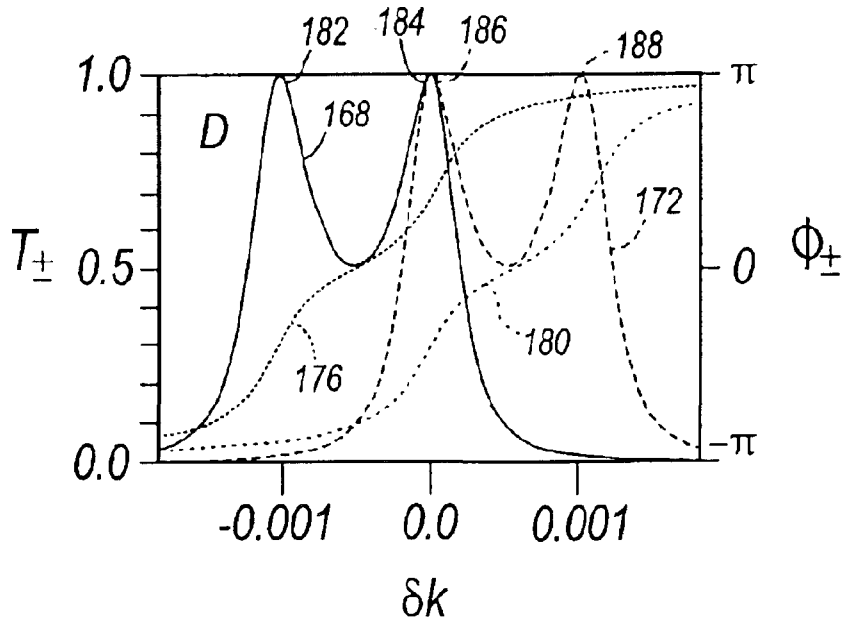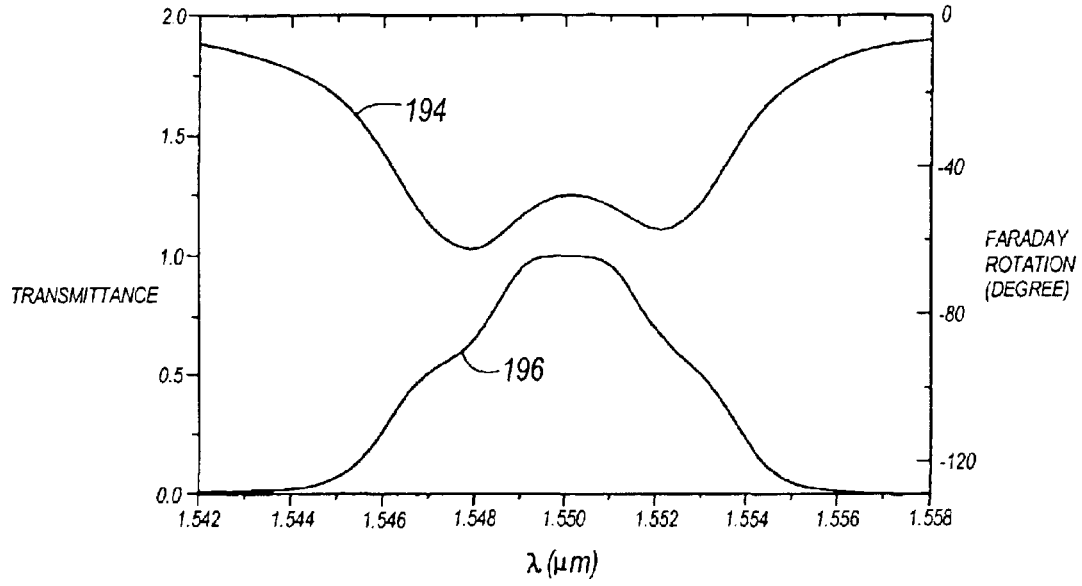
424

420

FIG. 15

1

MAGNETO-PHOTONIC CRYSTAL ISOLATORS

RELATED APPLICATIONS

This patent application claims the benefit of U.S. Provisional Patent Application No. 60/272,100, entitled "MAGNETO-PHOTONIC CRYSTAL ISOLATORS", filed on Feb. 28, 2001, the entire contents of which is incorporated herein by reference.

STATEMENT REGARDING FEDERALLY SPONSORED RESEARCH FOR DEVELOPMENT

This invention was made with United States government support under National Science Foundation awarded by the PHS grant number ECS 0115315. The United States government has certain rights in this invention.

BACKGROUND OF THE INVENTION

The present invention relates to photonic band-gap materials.

In many applications of lasers or other radiation sources, it is important to prevent reflected radiation from interacting with the source. Reflected radiation generates undesirable noise and unwanted f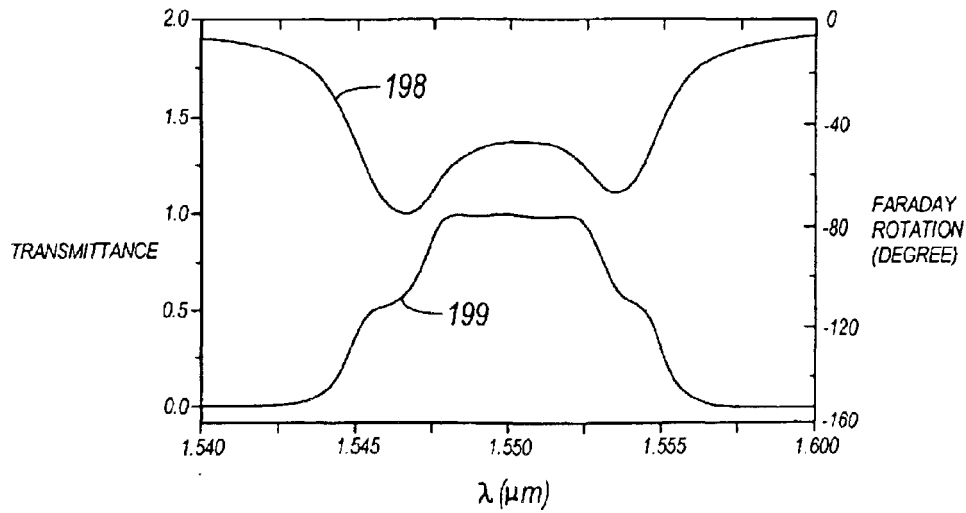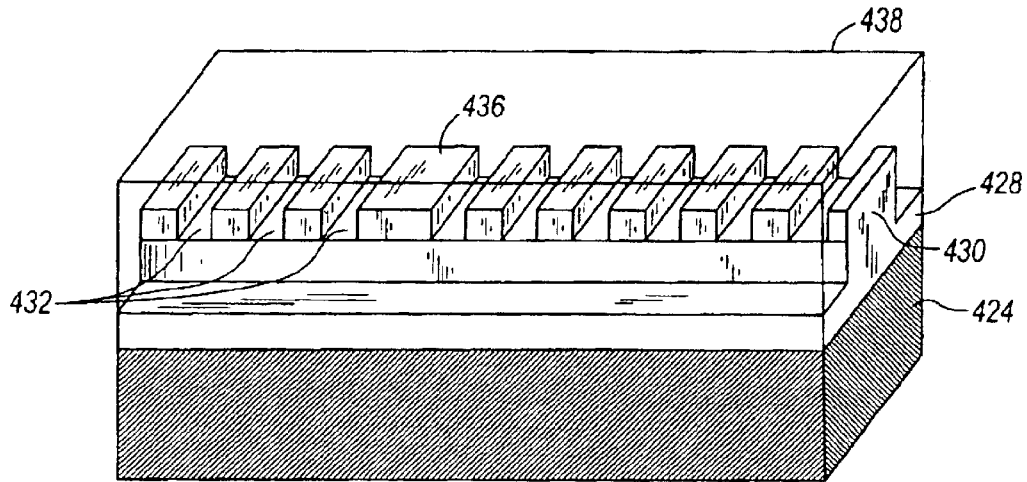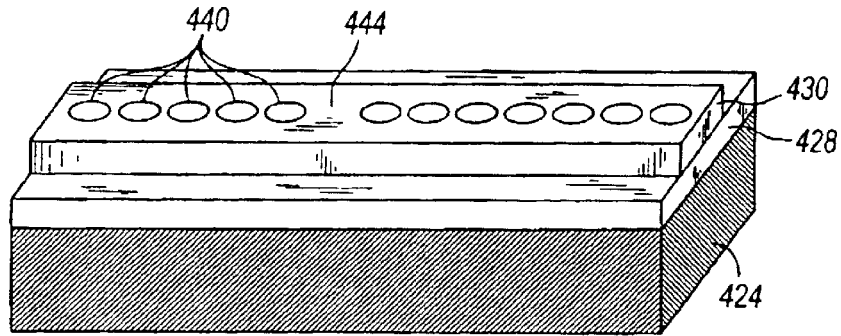eedback. Photonic or optical circuits is just one example of an application where there exists a need to isolate a source from reflected radiation.

As is known in the art, the Faraday effect in magneto-optical materials rotates the polarization of an incident beam as it passes through the material. Because of their Faraday effect, magneto-optical materials are used in non-reciprocal devices to serve as an isolator, i.e., a device that permits the transmission of light in only one direction. By placing an isolator near the radiation source in the path of propagating light, the isolator allows the emitted light to pass through. Any reflected light from the optical circuit is not permitted to pass through the isolator. Instead, the isolator blocks-out the reflected light, preventing the light from interacting with the source. However, traditional isolators are large, prohibiting them to be fabricated on an optical chip. A smaller isolator capable of being formed on an optical chip and produce a large Faraday rotation is thus desirable.

SUMMARY OF THE INVENTION

The invention provides a rotator formed from a photonic crystal capable of producing an enhanced Faraday rotation on an incident light beam. Photonic crystals, also referred to as photonic band-gap ("PBG") materials, are dielectric structures in which the refractive index changes periodically, creating a band gap at optical frequencies. The band gap forbids the propagation of a certain frequency range of light through the material. By introducing defects or resonant cavities in the PBG material, light can be localized or trapped in the defect. The material structure can be tuned to manipulate the light such that the material will induce resonant tunneling or the transmission of light.

In one embodiment, the invention provides a magneto-optical isolator for an optical circuit. The isolator includes first and second polarizers, and a photonic-crystal rotator. The rotator has at least one defect in the rotator and is positioned between the first and second polarizers. The rotator includes a magnetic material.

In another embodiment, the isolator includes a substrate, and an optical channel disposed next to the substrate. The optical channel and substrate are configured to transmit

2

optical radiation within the optical channel. The optical channel includes a photonic-crystal rotator. The rotator has at least one defect and includes a magnetic material.

In yet another embodiment, the invention provides a photonic-crystal rotator for an optical isolator. The rotator includes a substrate and an optical channel disposed next to the substrate. The optical channel and substrate are configured to transmit optical radiation within the optical channel. The optical channel includes a magneto-photonic band-gap material having a defect.

BRIEF DESCRIPTION OF THE DRAWINGS

FIG. 1 is a perspective view of an isolator embodying the invention.

FIG. 2 is a schematic diagram of an exemplary rotator included in the isolator shown in FIG. 1.

FIG. 3 is a schematic diagram of another exemplary rotator included in the isolator shown in FIG. 1.

FIG. 4 is a schematic diagram of yet another exemplary rotator included in the isolator shown in FIG. 1.

FIG. 5 illustrates the Faraday rotation in different rotators or stacks, which have a single defect and are operating in reflection.

FIG. 6 illustrates the transmission and phase of circularly polarized light for an exemplary two-defect rotator embodying the invention.

FIG. 7 illustrates the transmission and phase of circularly polarized light for another exemplary two-defect rotator.

FIG. 8 illustrates the transmission and phase of circularly polarized light for yet another exemplary two-defect rotator.

FIG. 9 illustrates the transmission and phase of circularly polarized light for even yet another exemplary two-defect rotator.

FIG. 10 illustrates the transmission and phase of circularly polarized light for an exemplary three-defect rotator.

FIG. 11 illustrates the transmission and phase of circularly polarized light for an exemplary four-defect rotator.

FIG. 12 is a schematic representation of a crystal being sliced by a crystal ion slicing method.

FIG. 13 is a perspective view of a film detached by the crystal ion slicing method.

FIG. 14 is a perspective view of another embodiment of a rotator embodying the invention.

FIG. 15 is a perspective view of yet another embodiment of a rotator embodying the invention.

DETAILED DESCRIPTION

Before any embodiments of the invention are explained in detail, it is to be understood that the invention is not limited in its application to the details of construction and the arrangement of components set forth in the following description or illustrated in the following drawings. The invention is capable of other embodiments and of being practiced or of being carried out in various ways. Also, it is to be understood that the phraseology and terminology used herein is for the purpose of description and should not be regarded as limiting. The use of "including," "comprising," or "having" and variations thereof herein is meant to encompass the items listed thereafter and equivalents thereof as well as additional items.

A magneto-optical isolator 20 embodying the invention is illustrated in FIG. 1. The isolator 20 includes a thin-film photonic-crystal stack or rotator 24 found in between a first

film polarizer **28** and a second film polarizer **32**. As shown in FIG. **1**, the rotator **24** and the polarizers **28** and **32** are three separate elements. In other embodiments, the rotator **24** and the polarizers **28** and **32** form a single element. An example polarizer **28** or **32** is a commercially fabricated film polarizer that is sold under the brand name Lamipol.

The rotator **24** includes periodic stacks of alternating magnetic and non-magnetic thin-film layers. As shown in FIG. **2**, the exemplary rotator **24** includes a first stack **36** of thin-film layers and a second stack **40** of thin-film layers. The first stack **36** alternates non-magnetic layers **44** with magnetic layers **48**, while the second stack **40** alternates magnetic layers **48** with non-magnetic layers **44**. The non-magnetic layers **44** have a first index of refraction, n_n, while the magnetic layers **48** have a second index of refraction, n_m, that differs from the first index of refraction. The magnetic layers **48** are formed from magnetic-garnet materials such as yttrium iron garnet ("YIG"), bismuth-substituted YIG ("Bi:YIG"), bismuth-substituted dysprosium iron garnet ("Bi:DyIG"), cerium-substituted YIG ("Ce:YIG"), ytterbium iron garnet ("YbIG"), bismuth-substituted YbIG ("Bi:YbIG"), or other various rare-earth iron garnets. These magnetic layers **48** have non-reciprocal properties, low losses, and large Faraday rotation in the near infrared region of the optical spectrum. However, other magnetic materials may be used with the invention. The magnetic material yields a larger Faraday rotation with a higher bismuth or other various rare-earth iron garnets content. The non-magnetic layers **44** are formed from materials such as gadolinium gallium garnet ("GGG"), silicon dioxide ("SiO$_2$"), tantalum oxide ("Ta$_2$O$_5$"), dysprosium gallium garnet ("DyGG"), neodymium gallium garnet ("NdGG"), or other non-magnetic dielectric materials. The magnetization of the magnetic layers **48** is oriented preferentially normal to the plane of the film.

The stacks **36** and **40** are configured such that when the first stack **36** is positioned next to the second stack **40**, a magnetic layer **48** from the first stack **36** is positioned next to a magnetic layer **48** from the second stack **40**. This configuration causes a variation in the periodicity of the rotator **24**. Two layers of the same material positioned next to each other without having a layer of differing material between them is referred to as a phase shift or a defect in the rotator. In other words, defects are introduced by varying or breaking the periodicity of the crystal. Varying the periodicity of the crystal may be accomplished by adding or removing one or more layers, or varying the length of one or more layers. As will be discussed below, the layers **44** and **48** can be manufactured using liquid phase epitaxy or radio frequency sputtering techniques. However, other manufacturing techniques are possible.

As shown in FIG. **2**, the rotator **24** has a single defect **52** positioned at the center of the rotator **24**, and is referred to as a symmetric magneto-photonic rotator. As shown in FIG. **3**, the rotator **60** also has a single defect **64**, however the defect **64** is not positioned near the center. Rotator **60** is referred to as an asymmetric rotator.

In some embodiments, the rotator **24** includes any number of stacks, resulting in numerous defects. As shown in FIGS. **2** and **3**, the rotators **24** and **60** include two stacks each, and each rotator **24** and **60** can be expressed as the form of $(NM)^j(MN)^k$, where N represents a non-magnetic layer and M represents a magnetic layer. The $(NM)^j$ series represents the first stack **36** and the $(MN)^k$ series represents the second stack **40**. The repetition factors j and k can vary independently, producing stacks of various lengths and symmetries, such as the symmetric rotator **24** or the asym-

metric rotator **60**. As shown in FIG. **4**, the rotator **72** includes three stacks **76**, **80** and **84** resulting in two defects **88** and **92**. The rotator **72** takes the form $(NM)^j(MN)^k(NM)^j$, where the first $(NM)^j$ series represents the first stack **76**, the $(MN)^k$ series represents the second stack **80**, and the second $(NM)^j$ series represents the third stack **84**. By increasing or decreasing j and k, the position of the defects can vary and result in producing symmetric rotators, such as rotator **24** or **72**.

As mentioned previously, the presence of a defect in the rotator **24**, **60**, or **72** introduces transmission resonances in the band gap that are associated with the trapped states of light. Also, patterning the rotator **24**, **60**, or **72** with alternating layers **44** and **48** of varying refraction indices produces a longer mean optical path length than in a uniform medium or material of the same length. As used herein, the term "optical path length" is the product of the geometrical distance of the layer and the refractive index. Therefore, the light tuned at or near the resonance in the band gap is largely transmitted. Yet, light trapped in the periodic rotator **24**, **60**, or **72** has a larger optical path length to overcome. In the periodic rotator **24**, **60**, or **72**, the circular birefringence effects the light over a longer mean optical path length, which in turn produces larger phase differences between the two circularly polarized beams. As used herein, the term "circular birefringence" is the separation of a light beam into two beams with opposite circular polarization, i.e. left-hand circularly polarized and right-hand circularly polarized. Half of the phase difference between right-hand and left-hand circular polarization determines the Faraday rotation of the structure. Thus, a larger phase difference produces an enhanced rotation. In other words, the periodic rotator **24**, **60**, or **72**, which produces a large optical path length over a relatively small geometric distance, yields a large enhanced rotation in the light beam while decreasing the physical length of the rotator **24**, **60**, or **72**.

A rotator that has only a single, central defect **52**, such as rotator **24**, is able to produce enhanced rotation in the light (due to the increase mean optical path length created by the layers **44** and **48**), but is accompanied with decreased transmission. Having the rotator **24** operate as a reflector produces the same rotational enhancement with the same decreased results for reflection. Moving the single defect towards the front of the rotator, as shown in FIG. **3** with the rotator **60**, and place corrugation gratings near the rear **96** of the rotator **60**, the rear grating **96** of the rotator **60** turns into an almost essentially perfect reflector. In rotators of the form $(NM)^j(MN)^k$, such as rotator **60**, the rear grating **96** enforces reflection when j is less than k.

FIG. **5** shows the Faraday rotation in different rotators or stacks, which have a single defect and are operating in reflection, as a function of length. For FIG. **5**, L is the length of the magnetic part of the stack. This is the total length of the stack when the rear grating is also magnetic. L becomes slightly smaller when the rear grating of the stack is not magnetic. Solid line **100** corresponds to a periodic stack of Bi:YIG/GGG (Bi:YIG as the magnetic layer and GGG as the non-magnetic layer) with high refractive index contrast after the single defect. The stack represented by the solid line **100** has a grating coupling strength, κ, of 123. Dashed line **104** also corresponds to a periodic stack of Bi:YIG/GGG with a grating coupling strength, κ, of 123. However, the stack represented by the dashed line **104** has the same refractive index contrast on both sides of the defect. Fine dotted line **108** and coarse dotted line **112** correspond to corrugated slab waveguide of Bi:YIG material each with a single defect and having a grating coupling strength, κ, of 15. The slab represented by the fine dotted line **108** has a high refractive

index contrast after the defect and the slab represented by the coarse dotted line 112 has a low refractive index contrast after the defect. As illustrated in FIG. 5, the periodic stacks of Bi:YIG/GGG represented by solid line 100 and dashed line 104 produce a Faraday rotation close to 90°, while reducing the length of the stacks to approximately less than 30 μm.

The trade-off between the Faraday rotation and the transmission of light, which is present in single defect structures, such as rotators 24 and 60, is reduced when using periodic stacks with two or more defects, such as rotator 72. The rotator 72 having two defects 88 and 92 is able to vary the location of one defect 88 or 92 or both defects 88 and 92, such that the rotator 72 induces the largest phase difference between the left-hand circularly polarized ("LHCP") light beam and the right-hand circularly polarized ("RHCP") light beam, while allowing both light beams to resonantly transmit through the rotator 72.

Each circularly polarized ("CP") light beam has a transmission resonance as a function of wave vector, k (the vector whose direction is the direction of propagation and whose magnitude is given by the wave number, $2\pi/\lambda$). However, these resonances are not harmonious for the two polarizations. Rather, each circular polarization exhibits one or two resonance peaks that vary depending upon the values of the repetition factors, j and k, in the rotator 72. The presence of the two defects allows one to adjust the resonance peak positions (by adjusting the values of j and k) until maximum transmission is achieved simultaneously for each polarization at any desired rotation. As stated previously, the rotator 72 is of the form $(NM)^j(MN)^k(NM)^j$. By varying the repetition factors j and k, adjustments are made to the positions of the defects 88 and 92 within the rotator 72 as well as the length of the rotator 72.

As shown in FIGS. 6, 7, 8, and 9, the transmission and phase of the LHCP beam and the RHCP beam are manipulated when the repetition factors, j and k, are varied in a two defect stack. FIGS. 6, 7, 8, and 9 also depicts the transmission and phase of circularly polarized light as a function of detuning the equation

$$\delta k = 2\pi/(\lambda^{-1} - \lambda_0^{-1})$$

Detuning refers to the difference between the frequency (or wavelength) of the light beam and the resonant frequency (or resonant wavelength) of the rotator 72, where λ_0^{-1} is the resonant frequency of the rotator 72, and λ^{-1} is the frequency of the light beam. Furthermore, each two-defect rotator corresponding to FIGS. 6–9 include alternating layers of magnetic and non-magnetic material 48 and 44. Each layer 44 and 48 is approximately a quarter-wave plate, with a thickness of

$$t_i = \lambda_0/4\sqrt{\epsilon_i}$$

where ϵ_i is the dielectric constant, i=M, N, and λ_0 is the resonant wavelength.

FIG. 6 illustrates the phase and transmission functions of each CP beams in a two-defect rotator having the ratio of repetition factor, j, to repetition factor, k ("j/k"), be 0.5. Solid line 120 and dashed line 124 represent the transmissions of LHCP light and RHCP light, respectively. Fine dotted line 128 and coarse dotted line 132 represent the phases of LHCP light and RHCP light, respectively.

FIG. 7 illustrates the phase and transmission functions of each CP beams in a two-defect rotator having the ratio of j/k be 1.0. Solid line 136 and dashed line 140 represent the transmissions of LHCP light and RHCP light, respectively.

Fine dotted line 144 and coarse dotted line 148 represent the phases of LHCP light and RHCP light, respectively.

FIG. 8 illustrates the phase and transmission functions of each CP beams in a two-defect rotator having the ratio of j/k be 0.77. Solid line 152 and dashed line 156 represent the transmissions of LHCP light and RHCP light, respectively. Fine dotted line 160 and coarse dotted line 164 represent the phases of LHCP light and RHCP light, respectively.

FIG. 9 illustrates the phase and transmission functions of each CP beams in an optimal two-defect rotator having the ratio of j/k be 0.58. Solid line 168 and dashed line 172 represent the transmissions of LHCP light and RHCP light, respectively. Fine dotted line 176 and coarse dotted line 180 represent the phases of LHCP light and RHCP light, respectively.

As shown in FIGS. 6, 7, 8, and 9, at the Bragg resonance, when $\delta k=0$, the transmission of both polarizations are approximately equal. However, the phase difference between each CP beam, and thus the Faraday rotation, is rather small for the rotators corresponding to FIGS. 6–8.

In the embodiment illustrated in FIG. 9, the rotator includes alternating layers of Bi:YIG and GGG with a resonant wavelength, λ_0, at approximately 1.55 μm. The rotator is approximately 37 μm and induces a Faraday rotation on the order of approximately 55°. When SiO_2 is substituted for GGG, a Faraday rotation of approximately 45° is achieved with a transmission rate of about 98%. However, the total length of the rotator is approximately 15.3 μm, with repetition factor j equaling 9 and repetition factor k equaling 17. This corresponds to a total of 35 pairs of layers, or 70 layers.

Also illustrated in FIG. 9, each peak 182, 184, 186, and 188 of the transmission lines 168, and 172, respectively, is relatively thin and corresponds to a small detuning number. As a result, the rotator represented in FIG. 9 only allows light beams that vary slightly in frequency from the resonant frequency of the rotator transmit at a high percentage. By manipulating the repetition factors, peaks 182 and 184 can form into a single peak, such as peak 190 in FIG. 6, and peaks 186 and 188 can form into another single peak, such as peak 192 in FIG. 6. Both peaks 190 and 192 are wider, and thus correspond to larger bandwidths for the rotator of FIG. 6. However, the difference in phase between the CP beams, illustrated as lines 128 and 132, is small, causing a small Faraday rotation.

However, with an introduction of a third or fourth defect in a rotator, the rotator is able to increase the Faraday rotation, while increasing the bandwidth near perfect transmission. FIGS. 10 and 11 illustrates transmission and Faraday rotation of a rotator with three defects and four defects, respectively. The rotator with three defects takes the form of $(NM)^j(MN)^k(NM)^k(MN)^j$, and the rotator with four defects takes the form of $(NM)^j(MN)^k(NM)^l(MN)^k(NM)^j$, where l is an additional repetition factor.

The rotator corresponding to FIG. 10 has the repetition factors of j equaling 13 and k equaling 28. The bandwidth, represented by solid line 194, for this rotator is approximately 2 nm for a Faraday rotation of approximately 45°. The Faraday rotation is represented by solid line 196. The rotator corresponding to FIG. 11 has the repetition factors of j equaling 12, k equaling 25, and l equaling 27. The bandwidth, represented by solid line 198, for the rotator with four defects is approximately 4 nm for a Faraday rotation of approximately 45°, as well. The Faraday rotation is represented by solid line 199.

In the embodiments shown, liquid-phase epitaxy ("LPE") or radio frequency ("RF") sputtering techniques are used to

grow the thin film magnetic and non-magnetic layers **48** and **44**, included in the rotators **24**, **60**, and **72**, on garnet templates. Crystal ion slicing is used to remove layers **44** and **48** from their deposition template. Crystal ion slicing employs the formation and etching of a sacrificial layer in bulk, epitaxially grown or sputtered films. Deep ion implantation is used to generate a damage layer several microns beneath the bulk layer surface. The lattice damage in this layer induces a large etch selectivity relative to the rest of the material. This damage allows a thin layer to separate from the bulk. The etchant used for magnetic oxides is phosphoric acid.

To prepare the sample for crystal ion slicing, helium or hydrogen ions, energized up to 4 MeV, are implanted nearly normal to the ferrite surface without masking. Implantation dosages range from approximately 1×10^{16} ions/cm^{-2} to approximately 1×10^{17} ions/cm^{-2}. The energy of the implantation can be adjusted to select the film thickness.

Helium or hydrogen is generally chosen as the implantation species because of their small atomic mass, thus yielding a deeply buried damage layer. Two dominant mechanisms for energy loss determine the implantation profile and the distribution of lattice damage in the crystal. At high ionic energies, the energy loss is dominated by electronic scattering. This process is adequately described by the Lindhard-Scharff-Schiott theory ("LSS theory"), which predicts a stopping power proportional to $E^{1/2}$. Here, E is the energy of the implanted ion along its trajectory. This process generates very little damage over most of the implant depth. At low energies, the stopping power is mostly due to Rutherford scattering with the host nuclei generating significant lattice damage. The nonlinear dependence on ionic energies ensures that the majority of the ions are deposited over a relatively narrow spatial region of the sample, where lattice defects are introduced by the transfer of energy to the target nuclei.

A schematic representation of the crystal ion slicing is shown in FIG. **12**, and an approximately 10 μm-thick YIG film detached in this manner is shown in FIG. **13**. A bulk stack **200** of magnetic material, non-magnetic material, or both is grown on a deposition template **202**, such as GGG or another substrate. The bulk stack **200** is implanted with helium or hydrogen ions **104**. The ions **204** penetrate the bulk stack **200** creating a damaged layer **208**. A thin layer **212** on top of the damaged layer **208** is able to be separated from the bulk stack **200**. In the embodiment shown, the thin layer **212** is a single non-magnetic layer **44** or magnetic layer **48** (as shown in FIGS. **2**–**4**). In other embodiments, the thin layer **212** is a stack of magnetic and non-magnetic layers, such as the stacks **36**, **30**, **76**, **80**, or **84** (as shown in FIGS. **3** and **4**), or is the multiple layers and stacks that form the rotators **24**, **60**, or **72**. A thin film **216** of YIG approximately 10 μm thick, shown in FIG. **13**, has been detached from a bulk stack (not shown) using the crystal ion slicing process.

The rotator **24**, **60**, or **72** is then inserted into an optical channel **350** (shown in FIG. **1**). For the embodiment shown, the rotator **24** is inserted into a narrow slot or opening **354** cut out in the channel **350** by reactive ion etching or chemically assisted ion beam etching. The first polarizer **28** is inserted into another slot **358** found on one side of the first slot **354**, while the second polarizer **32** is inserted into a third slot **362** found on the other side of the first slot **354**. A magnet or group of magnets are placed in close proximity to the rotator **24**. The magnet has a magnetic field that interacts with the channel **350**. In one embodiment, film magnets are placed on top of the channel **350**, and in another embodiment, film magnets are placed on either side of the

channel **350**. The magnets saturate the magnetization along the rotator **24** and channel **350** in the direction parallel to a channel axis **1**—**1**.

During operation, light emitted from a laser, a light emitting diode (LED), or another suitable source travels through the channel **350** and is incident on the first polarizer **28**. The first polarizer **28** allows the emitted light having the same polarization as the first polarizer **28** to pass through. The emitted light is then incident of the rotator **24** and while it passes through, the rotator **24** rotates the polarization of the emitted light by approximately 45°. The emitted light is then incident on the second polarizer **32**, which allows the emitted light that has been previously adjusted by the rotator **24** to transmit through. Any light that passes through the second polarizer **32** and is reflected by other components of an optical circuit then passes through the polarizer **32**, and suffers another 45° rotation by the rotator **24**. Therefore, the reflected light incident on the rotator **24** is not transmitted through the rotator **24**, because its polarization direction is at 90° to the polarization axis of polarizer **28**.

In another embodiment illustrated in FIGS. **14** and **15**, a rotator **420** takes the form of an optical channel within a waveguide that is fabricated on an optical circuit chip. In FIG. **14**, the rotator **420** includes a non-magnetic substrate **424**. In the embodiment shown, the substrate **420** is fabricated from GGG material or other suitably lattice-matched garnet materials, such as dysprosium gallium garnet (DyGG). In other embodiments, the substrate **420** uses the same non-magnetic materials as the non-magnetic layers **44** found in the rotators **24**, **60**, and **72**.

The rotator **420** also includes an optical channel **428** having a ridge **430** along axis **14**—**14**. The optical channel **428** in the embodiment shown is formed from a magnetic garnet material, such as Bi:YIG. In other embodiments, the channel **428** is formed from the same magnetic materials as the magnetic layers **48** found in the rotators **24**, **60**, and **72**. The channel **428** induces resonant tunneling of certain wavelengths of light by positioning a series of depressions on the ridge **430** of the channel **428**. As shown in FIG. **14**, the depressions are gratings or grooves **432** on the ridge **430**. The gratings **432** change the refractive index of the channel **428** and generate a periodic modulation in the refractive index disposed to create a photonic band-gap structure in the film. In the embodiment shown, the gratings **432** are patterned on the ridge **430** that are approximately 200 nm long. Defects are created in the channel **428** by skipping a depression or widening a depression. In the embodiment shown, a defect **436** is created when a groove is skipped.

In order to avoid spurious linear birefringence due to lattice mismatch stress, the optical channel **428** or magnetic garnet layer is suitably LPE-grown or sputtered onto a lattice-matched substrate. Thus, for example, a YIG film on GGG or YbIG on DyGG. The magnetization in the YIG film is preferably parallel to the channel axis **14**—**14** to avoid linear magnetic birefringence.

In other embodiments, the rotator **420** further includes a cover **438** of non-magnetic material, such as GGG, to create a symmetric structure by using a cover layer with nearly the same index of refraction as the substrate **424** to avoid geometrical or waveguide linear birefringence. In the embodiment shown, the same material is used for the substrate **424** and the cover **438** in order to eliminate any refractive index asymmetries between the cover **438** and substrate **424**.

In the embodiment shown in FIG. **15**, the depressions found in the channel **428** take the form of holes **440**. The channel **428** changes its refractive index by etching the holes

440 in the top of the ridge 430. These holes 440 are etched by reactive ion or chemically-assisted ion beam etching. Defects are created in this embodiment by leaving a larger gap, such as gap or defect 444, in between two holes 440. In other embodiments, the defects are produced by widening the holes or changing the shape and size of the holes. Also, in other embodiments, the rotator 420 includes multiple defects, rather than a single defect 436 or 444.

The rotator 420 is fabricated by liquid phase epitaxy or RF sputtering techniques to form and position the various layers. First, a layer of Bi:YIG or another suitable magnetic garnet is deposited over a non-magnetic substrate 424. As mentioned previously, in the embodiment shown, the substrate 424 is made from GGG or another suitably lattice-matched garnet material. The layer of Bi:YIG forms the optical channel 428. Using a phosphoric etch or similar etching technique, a ridge 430 is etched from the layer of Bi:YIG. In the embodiment shown, the ridge 430 is square in order to enhance the channel symmetry and minimize linear birefringence. In other embodiments, the ridge 430 is deposited as a layer on to the channel 428 using an RF sputtering technique. The gratings 432 or holes 440 are then patterned on the ridge 430 by electron-beam lithography, followed by reactive ion etching or chemically assisted ion beam etching. In the embodiment shown, the gratings 432 are approximately 200 nm. Once the gratings 432 or holes 440 have been patterned in the ridge 430, the cover 438 of non-magnetic material is sputtered over the channel 428.

In another embodiment, reactive dual ion beam sputtering ("RDIBS") is employed to produce Bi:YIG films on high-quality smooth thermally-grown SiO_2. RDIBS systems are used for the purpose of enhancing the refractive index contrast between film, substrate, and cover, then covered by smooth and dense RDIBS deposited SiO_2 layers with good optical properties. RDIBS allows the waveguide to shorten, since shorter planar photonic-crystal structures for optical isolation can be built. Thus, the gain is not only the reduction of size of the optical isolator devices, but the integration of the isolators onto silicon platforms.

Various features and advantages of the invention are set forth in the following claims.

What is claimed is:

1. A magneto-optical isolator for an optical circuit, the isolator comprising:

a substrate; and

an optical channel disposed next to the substrate, the optical channel and substrate being configured to transmit optical radiation within the optical channel, the optical channel including a photonic-crystal rotator, the rotator having at least one defect and including a magnetic material, and wherein the optical channel includes a series of depressions having a periodicity and wherein the defect includes a variation in the periodicity of the depressions.

2. An isolator as set forth in claim 1 wherein the isolator further comprises first and second polarizers.

3. An isolator as set forth in claim 1 and further comprising a magnet having a magnetic field, the magnet being positioned such that the field interacts with the rotator.

4. An isolator as set forth in claim 1 wherein the substrate, the optical channel, and the rotator form a monolithic photonic device.

5. An isolator as set forth in claim 1 wherein the optical channel is a magnetic material.

6. An isolator as set forth in claim 5 wherein the magnetic material is selected from the group consisting of yttrium iron garnet (YIG), bismuth-substituted YIG, bismuth-substituted dysprosium iron garnet, and cerium-substituted YIG.

7. A photonic-crystal rotator for an optical isolator, the rotator comprising:

a substrate; and

an optical channel disposed next to the substrate, the optical channel and substrate being configured to transmit optical radiation within the optical channel, the optical channel including a magneto-photonic band-gap material having a defect;

wherein the optical channel has an axis,

wherein the optical channel includes a series of depressions along the axis, the series of depressions having a periodicity, and

wherein the defect includes a variation in the periodicity of the depressions.

8. A rotator as set forth in claim 7 wherein the variation in the periodicity is a lack of at least one depression.

9. A rotator as set forth in claim 7 wherein the depressions are holes within the optical channel.

10. A rotator as set forth in claim 9 wherein the variation in the periodicity is a lack of at least one hole.

11. A rotator as set forth in claim 7 wherein the optical channel includes a series of grates along the axis,

wherein the depressions are formed by the grates.

12. A photonic-crystal rotator for an optical isolator, the rotator comprising:

a substrate; and

an optical channel disposed next to the substrate, the optical channel and substrate being configured to transmit optical radiation within the optical channel, the optical channel including a magneto-photonic band-gap material having a defect, wherein the optical channel has an axis,

wherein the optical channel includes a series of grates along the axis, the series of grates having a periodicity, and

wherein the defect includes a variation in the periodicity of the grates.

13. A rotator as set forth in claim 12 wherein each grate has a length in the direction of the axis, and

wherein the variation in the periodicity is a variation in the length of at least one of the grates.

14. A photonic-crystal rotator for an optical isolator, the rotator comprising:

a substrate; and

an optical channel disposed next to the substrate, the optical channel and substrate being configured to transmit optical radiation within the optical channel, the optical channel including a magneto-photonic band-gap material having a defect, wherein the optical channel has an axis,

wherein the optical channel includes a slab and a ridge disposed on the slab, the ridge being in a direction of the axis,

wherein the ridge includes a series of depressions along the axis, the series of depressions having a periodicity, and

wherein the defect includes a variation in the periodicity of the depressions.

15. A rotator as set forth in claim 14 wherein the slab and the ridge are unitary.

16. A photonic-crystal rotator for an optical isolator, the rotator comprising:

a substrate; and

an optical channel disposed next to the substrate, the optical channel and substrate being configured to transmit optical radiation within the optical channel, the optical channel including a magneto-photonic band-gap material having a defect, wherein the optical channel has an axis,

11

wherein the optical channel includes a slab and a ridge
disposed on the slab, the ridge being in a direction of
the axis,

wherein the optical channel further includes a series of
grates disposed on the ridge along the axis, the series of
grate having a periodicity, and

12

wherein the defect includes a variation in the periodicity
of the grates.

17. A rotator as set forth in claim **16** wherein the slab, the
ridge, and the grates are unitary.

* * * * *